Quality assurance in bored PHC nodular piles through control of design capacity based on loading test data

1.24

Madan B. Karkee — Manager, Research Division, GEOTOP Corp., Tokyo, Japan
Shigeo Kanai — Manager, Development Division, GEOTOP Corp. Tokyo, Japan
Takashi Horiguchi — Senior Managing Director, GEOTOP Corp., Tokyo, Japan

SYNOPSIS

Bored PHC nodular piles tend to be favourable foundation option for low to medium-rise buildings at deep soft ground conditions. This paper attempts to develop a rational formulation to evaluate the vertical load bearing resistance of these piles based on a comprehensive field loading test program. For a global safety factor of 3.0 currently applicable in Japanese practice, a reliability index β of 4.9, significantly larger than 3.2 suggested in such cases, is obtained for the formulations proposed. When β of 3.2 is considered acceptable, a safety factor of 2.0 is found to be adequate, showing the potential for significant improvement in design economy. A convenient approach to control the design capacity within a defined reliability level is proposed based on the loading test results.

INTRODUCTION

Probably little known elsewhere, precast nodular piles have been in use for more than six decades in Japan. Over the years, reinforced concrete nodular piles of rectangular, triangular, hexagonal and circular cross sections have been used. In recent years, prestressed precast high strength concrete (PHC) nodular piles of circular cross section have been common. The diameter (D_a) of pile shaft is relatively small, while the nodal diameter (D) generally varies from 1.25 to 1.40 times D_a. High strength concrete of grade 80MPa or 85MPa and effective prestress levels of 4MPa, 8MPa or 10MPa are used depending on the type classification conforming to the JIS specification. The PHC nodular piles are generally used to support low to medium-rise buildings at locations with deep soil deposit, where the competent bearing stratum is very deep. Thus the piles are embedded in relatively soft surficial deposits, and a major portion of the vertical resistance is derived from shaft resistance. In this sense, the PHC nodular piles are commonly referred to as friction piles.

This paper is concerned with the development of a rational and reliable approach to the design of PHC nodular piles based on the results of loading test and in conjunction with soil parameters readily available from common exploration boring practice. In Japan, the parameters available for the design of pile foundation at a site is most often limited to the standard penetration test (SPT) N-value and the soil type classification. This is particularly so in case of small to medium size construction projects where the bored PHC nodular piles are generally used. The results of an extensive field loading test program on fully instrumented bored PHC nodular piles is analysed in detail to arrive at a rational method for evaluation of the vertical resistance. Altogether 51 loading test data covering different ground conditions throughout Japan are utilised to develop a simple correlation that can be readily employed in the design practice. The correlation of unit nominal frictional resistance ζ with average N-values were developed for three broad types of soil comprising *sand*, *clay* and *humus*. For toe resistance *q*, a single correlation with average N-value around pile toe (N_P) was considered irrespective of the soil type. However, it was noted that the soil near pile toe was of sandy type in most of the 51 loading test cases. Reliability of the proposed correlation equations was investigated to show that the proposed method of evaluating the vertical bearing resistance can be employed in practice with adequate confidence.

METHOD OF PILE INSTALLATION

Traditionally, the nodular piles were installed by driving while maintaining a heap of gravel around the pile so as to have the annular space between the pile and the hole packed with the gravel. The resulting combination of the nodular pile with gravel all around was found to provide an efficient load bearing system. Following the strict stipulations against noise and vibration pollution in the seventies, installation of piles by driving in populated city areas of Japan was rendered practically unthinkable. One of the outcome of the search for alternate methods of installation was the extensive development of bored precast piles in Japan. The method is also referred to as preboring, and there are many variations in common use. In case of the PHC nodular piles considered in this study, the installation involves first drilling a vertical hole with an auger. Once the predetermined depth is reached, the auger is withdrawn along with the injection of cement grout (slurry). The volume of the grout is adjusted so as to fill the hole completely when the closed ended pile is inserted into it. The pile gets bonded to the ground as the cement grout hardens and gains strength with time. The pile thus installed is referred to as the *Bored PHC Nodular Pile*.

Two sizes of PHC nodular piles, designated as 440-300 and 500-400 in Fig. 1, were used in this study. The size designation follows the format D-D_a. The respective drilled hole diameter (D_b), pile axis diameter (D_a) and the pile nodule diameter (D) are also given in Fig.1.

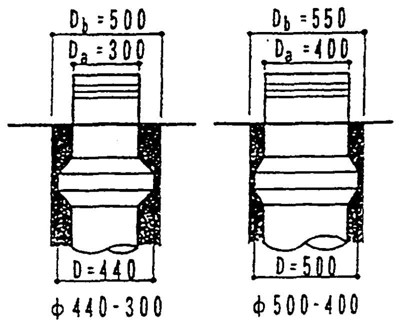

Fig. 1 PHC Nodular Pile Sizes

Extent of Displaced Soil from Drilling

Two types of augers are generally used in bored PHC nodular pile. One is the normal multiple flight auger in which the soil from the hole is fully displaced and needs to be disposed of from the project site. The other is a specially designed auger that reduces the soil displaced from the drilled hole. When this auger is employed, the soil around the drilled hole gets compacted resulting in reduction in the displaced soil to be disposed of. In either case, the diameter D_b of the drilled hole is 500mm for 440-300 size pile and 550mm for 500-400 size as shown in Fig.1. The reduction in the volume of displaced soil resulting from the use of specially designed auger is of the order of 30 to 60% depending on the soil condition.

Strength of the Hardened Cement Grout

It is clear that the bearing capacity of the bored PHC nodular pile is derived from the transfer of the load to the surrounding soil by the hardened cement grout. Consequently, the strength of hardened cement grout has to be at least superior to the surrounding soil. It is imperative that the grout be designed to have the adequate target strength and to ensure that desired strength is actually achieved in practice. In practice, cement grout of higher target strength is injected around the pile toe region in recognition of generally higher load transfer demands there. As a standard practice, the water-cement ratio (w/c) of the grout in the pile toe region is 100% and that around the pile shaft is 140%. The 28 day target strength is 7.5MPa and 3.0MPa respectively. Specimens of the cement grout from the cement slurry plant at the site were collected during installation of most of the 51 test piles considered in this study. The distribution of 28 day compressive strength (F_g) of the specimens are shown in Figs. 2 and 3, where a lognormal distribution is seen to be a close approximation to the distribution of data. (The form of probability density function for a lognormal distribution is given by Equation 1.) The probability of the grout strength exceeding the target strengths defined above was found to be 95% and 99% for w/c of 100% and 140% respectively.

To see if the strength of the cement grout hardened within the ground after pile installation met the target strength requirement, two 5m long bored PHC nodular piles installed using the two types of auger described above, were completely pulled out for close inspection after conducting pull out tests. Samples of hardened cement grout were cut out from the upper pile shaft and the pile toe regions and tested for unconfined compressive strength (F_{gcut}). For the pile toe region, F_{gcut} was found to be about 12.8MPa, which is larger than the mean value in Fig. 2, exceeding the target strength by a good margin. Similarly, F_{gcut} was about 3.8MPa for the upper shaft region, which, although less than the mean value, is still larger than the target strength of 3.0MPa as indicated in Fig. 3. Thus, it was confirmed that the actual strength of the grout hardened in the ground is higher than the target strength. It was also noted from the pull out test that cement grout was bonded well with the pile shaft.

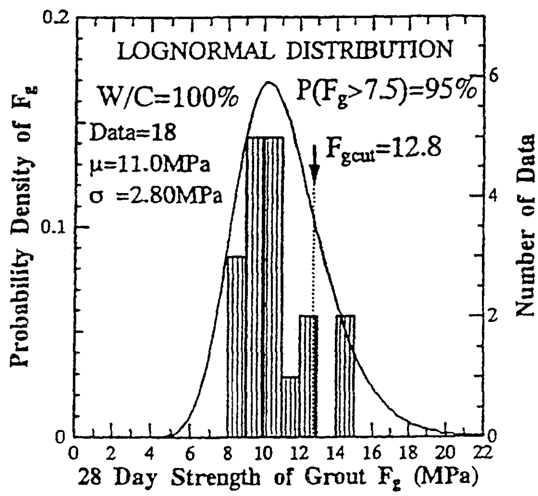

Fig. 2 Probability Density of Strength F_g of the Cement Grout with w/c=100%

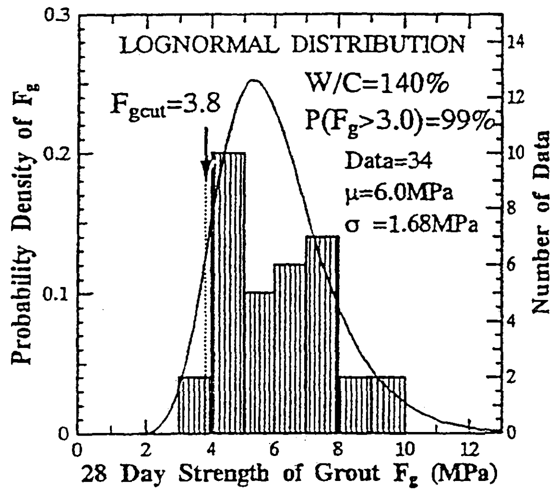

Fig. 3 Probability Density of Strength F_g of the Cement Grout with w/c=140%

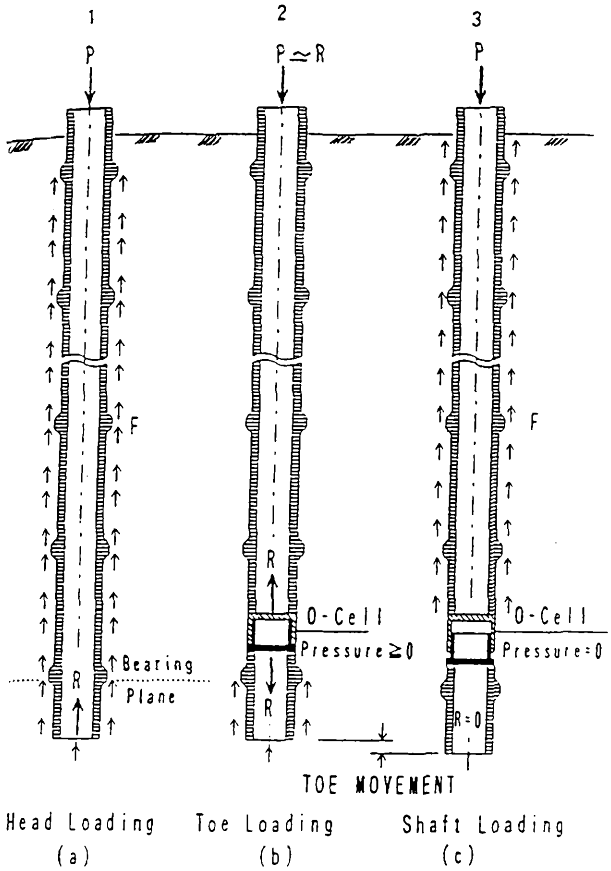

Fig.4 Head Loading Test and the Use of the O-Cell for Toe Loading & Shaft Loading Tests

LOADING TESTS ON FULLY INSTRUMENTED PILES

All the tests were conducted by applying the slow maintained loading based on the Japan Geotechnical Society (JGS) standard (3). The incremental loads were maintained at constant values for a period 30 minutes, and the load was cycled back to zero incrementally. The applied load, the pile head movement (S_0) and the pile toe movement (S_P) were measured directly. The axial force distribution was derived from the strain gage measurements at several points along the pile axis. The horizontal displacement of the pile head and the movement of reaction piles were monitored for accuracy of test results. Basically, the load was increased until the movement was at least 10% of the nodule diameter (D) or until creep deformations were excessively large to make maintaining the load difficult.

Separation of Pile Head Load into Shaft Resistance and Toe Resistance

The piles were fully instrumented to directly measure the resistance developed at different portions of the shaft and the toe, depending on the adjacent soil conditions, as the pile movement increases with the load applied at the head. The axial load distribution obtained from the strain gage measurement (2) can be readily used for this purpose. However, the resistance at different portions of the shaft and the toe tend to interact with each other under the action of the loading at the head. It is evident that the strain gage measurements include effects of such interaction effects. In addition, there is the inherent question of the accuracy of the force components measured by strain gage records. Osterberg load cell (O-cell) was utilised to investigate the extent of such effects and to verify that such effects were of minor consequence from practical point of view.

Use of O-Cell for Toe Loading and Shaft Loading Tests

As indicated in Fig.4(a), the "head loading" involves application of the load at the pile head by jacking against the reaction frame anchored to the ground by reaction piles. The conventional O-cell method (4) involves a hydraulic jack usually installed near the pile toe, such that when loaded the pile shaft is pushed upward against the pile toe, thus doing away with the need for the reaction frame system. However, in this study the O-cell is used in combination with the reaction frame system for "Toe Loading" and "Shaft Loading" tests as illustrated in Fig.4(b) and (c) respectively.

Toe loading involved application of load directly to the pile toe while keeping the pile shaft from being pushed upward by holding the head fixed by jacking against the reaction frame, so that no shaft resistance was allowed to develop. The two jacks, one at the head and other at the toe, were operated synchronously for this purpose. Once the toe loading test was completed, the pressure in both the jacks was released simultaneously to completely free the lower end of the pile as shown in Fig.4(c). Under this condition, the shaft loading was carried out by loading the pile head downward against the reaction frame. This way, the shaft resistance against downward movement was directly measured without interference with the pile toe movement.

COMPARISON OF THE RESULTS OF HEAD, TOE AND SHAFT LOADING TESTS

Three pair of tests were carried out at two sites (designated Site-A & Site-B) to compare the shaft and toe resistance measured independently by using the O-cell, with those obtained from the head loading test and strain gage reading, other conditions remaining the same. Fig.5 shows a pair of bored PHC nodular piles at site-A, where the pile P2 is shown to be fitted with the O-cell and circled numbers show the axial layout of a set of either 2 or 4 diametrically opposite strain gages at different levels. Head loading test was carried out on P1, while the toe loading and shaft loading tests were conducted on P2.

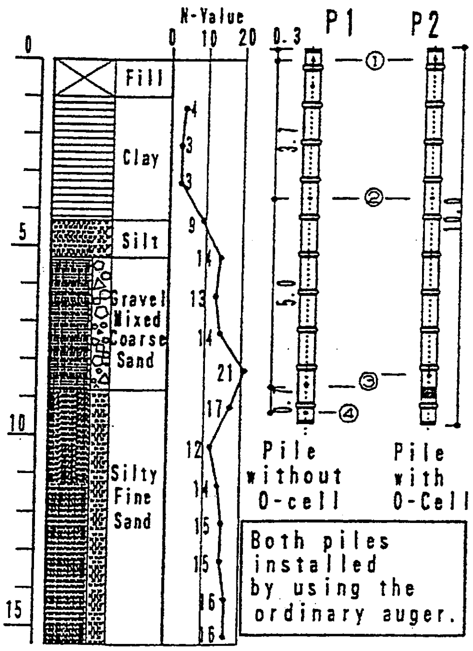

Fig.5 Pairs of Bored PHC Nodular Piles at the Site-A for Head, Shaft & Toe Loading Tests

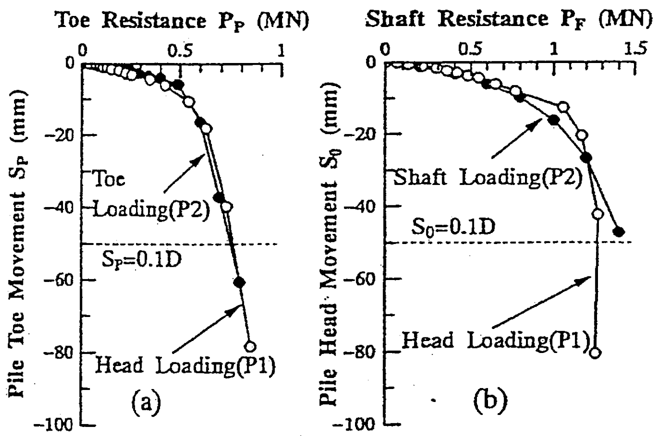

Fig.6 Comparison of Toe and Shaft Resistance from the Head Loading with those from the Toe and Shaft Loading Tests at Site-A

Fig.6(a) compares the toe resistance P_P measured from the head and the toe loading tests on the piles P1 and P2 respectively. Very good agreement of the pile toe movement curve obtained by the two tests can be noted indicating good reliability of the strain gage measurement in head loading test. Similarly, the shaft movement curve in Fig.6(b) obtained from the head loading compares well with that from the shaft loading. The agreement is particularly good within the pile head movement of about 20mm.

Fig.7 shows a set of four test piles (numbered 1 to 4) at the site-B. All the piles were instrumented similarly except that piles 3 & 4 were fitted with the O-cells. Again, the circled numbers show the strain gage layout. Piles 1 & 3 were installed by using the ordinary auger, in which most of the soil from the drilled hole is displaced, while piles 2 & 4 were installed by using the special auger, discussed above, in which the displaced soil is reduced by pressing and compacting the soil around the hole during the drilling operation. The head loading tests (piles 1 & 2) and the toe loading followed by the shaft loading (piles 3 & 4) tests were conducted as described above.

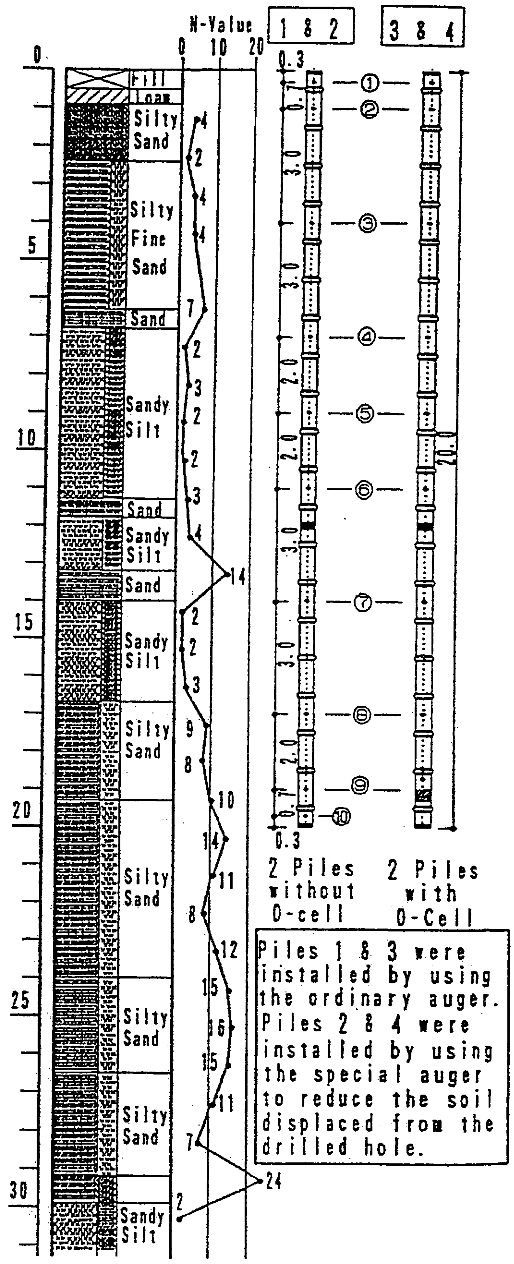

Fig.7 Two Pairs of Bored PHC Nodular Piles at Site-B for Investigation of Shaft & Toe Resistance components

Fig.8 shows the comparison of pile toe movement curves obtained by head loading and toe loading at site-B. Similarly, Fig.9 compares the shaft movement from the head loading and the shaft loading for the corresponding cases. The movement curves from the head loading test obtained by strain gage measurement compare well with those directly obtained by toe loading and shaft loading tests. The comparisons in Figs.6, 8 and 9 demonstrate the validity and reliability of the use of strain gage measurement to evaluate the axial force distribution in the 51 head loading tests utilised in this study.

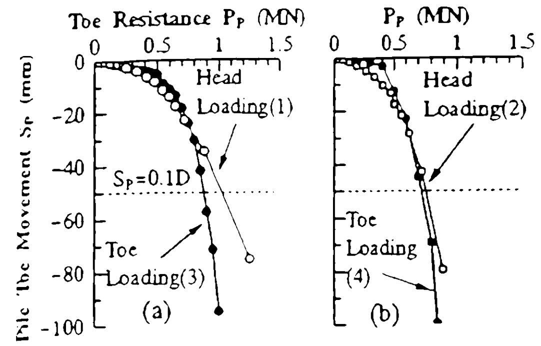

Fig.8 Comparison of Pile Toe Movement Curves from the Head Loading and the Toe Loading Tests at Site-B

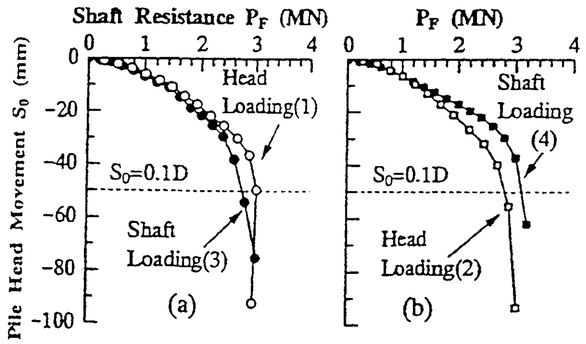

Fig.9 Comparison of Pile Shaft Movement Curves from the Head Loading and the Shaft Loading Tests at Site-B

Effect of the Reduction in Displaced Soil on the Shaft Resistance

Of the 51 load test data utilised in this study, 22 involve the use of the special auger to reduce the volume of soil displaced from drilling. The reduction in the displaced soil results from the improvement of the soil surrounding the hole by compaction. As a consequence, some increase in the shaft resistance and hence in the bearing capacity may be expected.

A pair of shaft loading tests on two piles (3 and 4) at site-B shown in Fig.7, one installed by an ordinary auger and the other by the special auger, were utilised to investigate the nature and the extent of increase in the shaft resistance. The shaft resistance for piles 3 and 4 of Fig.7 are compared in Fig.10. It can be seen that the shaft resistance is larger for the pile installed to reduce the displaced soil (pile 4), and that the increase is particularly prominent at larger values of shaft movement.

However, the increase is not significant at pile head movement of less than about 10mm, the range that corresponds to the service loads generally expected in practice. The soil condition at site-B being primarily of sandy type, the increase in the shaft resistance was expected to be appreciable. In fact, an increase of about 15% in shaft resistance can be noted at S_0=0.1D in Fig.10. Considering that the increase in the shaft resistance due to reduction in the displaced soil is rather insignificant at expected service load situations, it was considered insignificant to attempt quantification of the possible increase in bearing capacity. Consequently, all the 51 load tests on bored PHC nodular piles are considered together, irrespective of the extent of displaced soil from drilling operation.

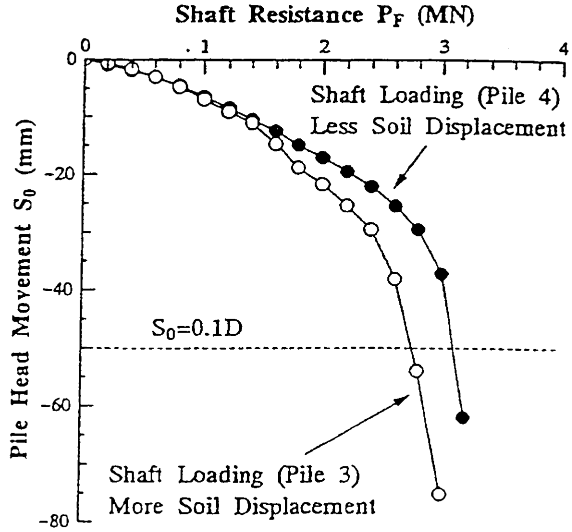

Fig.10 Effect of Reduction in Displaced Soil from Drilled Hole on the Shaft Capacity.

ANALYSIS OF LOADING TEST RESULTS

The JGS standard (3) defines ultimate resistance (R_m) obtained from loading test as smaller of the pile head load (P_0) at a pile toe movement (S_P) of 10% of the pile diameter and the load at which the movement curve may be regarded as parallel to the movement axis. In case of bored PHC nodular pile, three possible definitions of pile diameter exist, as denoted by D_a, D and D_b in Fig.1. Nodal diameter D was used in this regard because the lowest node of the pile (see Figs.5 & 7) is considered to provide the toe bearing area. There were only 9 loading tests out of the total of 51 in which the pile head movement did not reach 10% of D, and it was noted that none of the movement curves tended to be parallel to the movement axis.

Ultimate Resistance and Its Distribution Along the Pile Shaft

In this study, the measured ultimate resistance (R_m) was obtained as the value of P_0 at S_0=0.1D. In 9 cases where S_0 did not reach 10% of D because further load strength of the pile, R_m was estimated by extrapolation using the hyperbolic movement curve fitted to the measured data. Next, the distribution of R_m along the pile length was determined based on the strain gage measurements.

Unit Shaft Resistance ζ and Unit Toe Resistance q
From the axial distribution of the total resistance R_m, the share of the different sections of the shaft and that of the toe was evaluated. The different sections of the shaft considered correspond directly to the strain gage measurement intervals, such as those indicated by circled numbers in Figs.5 & 7. The cement grout that bonds the bored PHC nodular pile shaft to the surrounding ground is of considerably higher strength compared to generally soft soils it is in contact with, and it is logical to consider the slippage to occur at the interface between the soil and the hardened grout. The slippage at this interface was actually confirmed by the pull-out tests mentioned above. Consequently, the unit shaft resistance ζ is computed based on the hole diameter D_b (Fig.1). As also mentioned above, the unit toe resistance q is computed based on the nodal diameter D.

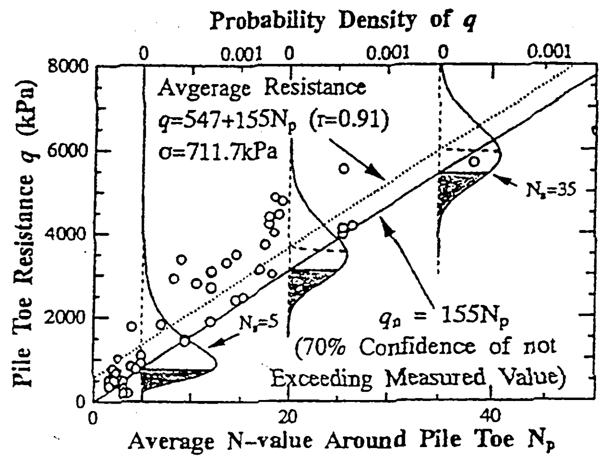

Fig.11 Correlation for Pile Toe Resistance q

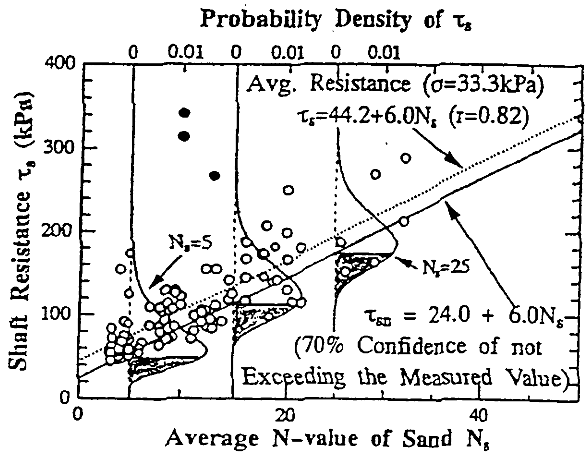

Fig.12 Unit Shaft Resistance in Sand τ_s

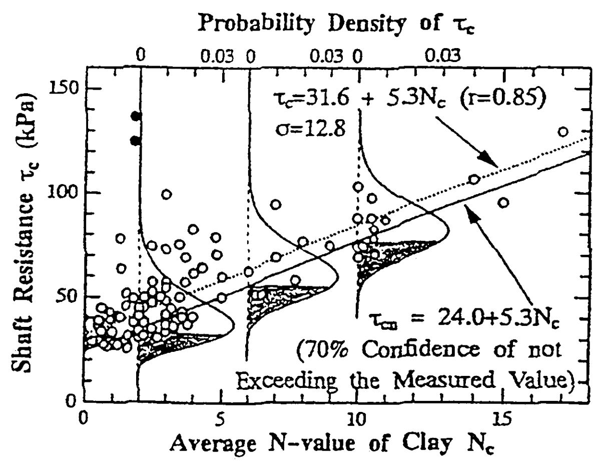

Fig.13 Unit Shaft Resistance in Clay τ_c

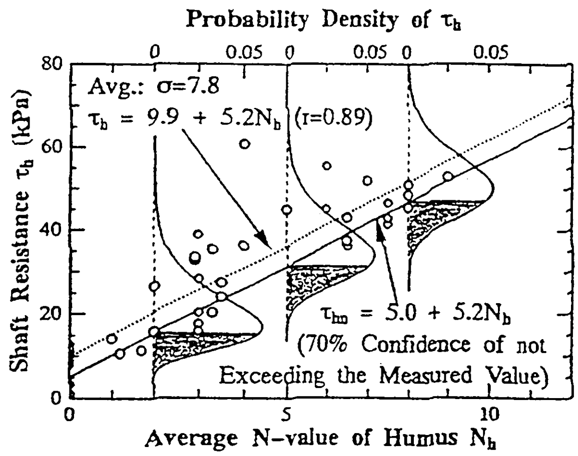

Fig.14 Unit Shaft Resistance in Humus τ_h

Determination of Soil Parameters

The ground condition shown in Figs.5 and 7 are typical of the situation where bored PHC piles are frequently employed. The soil types within different gage intervals were broadly classified as either sand, clay or humus, depending on the major content. The corresponding average SPT N-values of the intervals were designated as N_S, N_C and N_h respectively. The unit shaft resistance of the different intervals were computed based on strain gage readings and designated as ζ_S, ζ_C or ζ_h, depending on whether the soil type was sand, clay or humus respectively. The N-value N_P of the pile toe region was determined as the average in the region between 1.0D above and 1.0D below the nodule near the lower end, without any regard to the soil type. The soil type in the pile toe region, however, was mostly sandy type.

CORRELATION OF RESISTANCE WITH SOIL PARAMETERS

Fig.11 shows the plot of the unit toe resistance (q) with N_P, where a tendency for a fairly good linear correlation can be noted. Similarly, Figs.12, 13 and 14 show the plots of τ_s, τ_c and τ_h with respect to N_S, N_C and N_h respectively. Although some of the data are significantly large, a tendency towards a linear relation can be noted in all cases. A simple linear regression was carried out to fit a straight line of the form $y=a+bx$ to the data in all the four cases.

The average relation thus obtained are shown by the doted line in Figs.11 to 14. Three data points in Fig.12 and two data points in Fig.13, all denoted by black dots, were disregarded while fitting the line to the data. The correlation coefficient r and the standard deviation σ are also shown in Figs.11 to 14. The value of r is found to vary from about 0.8 for τ_c to about 0.9 for q, indicating a fairly good correlation.

Lognormal Distribution of Resistance

Considering that the distribution of the data above and below the average lines in Figs.11 to 14 tend to be skewed with larger dispersion above, it was considered reasonable to assume a lognormal distribution of the data. The probability density of the resistance R considering a lognormal distribution is given by Equation 1.

$$f_R(R) = \frac{1}{\sqrt{2\pi}\;\zeta R}\exp\left[-\frac{1}{2}\left(\frac{\ln R-\lambda}{\zeta}\right)^2\right] \qquad 0 \le R < \infty \tag{1}$$

In Equation 1, λ is the mean of lnR and ζ is standard deviation of lnR., R being either q, τ_s, τ_c or τ_h depending on the case under consideration. In terms of the mean μ and the standard deviation σ of R, the values of ζ and λ are given as:

$$\zeta = \sqrt{\ln\left(1+\frac{\sigma^2}{\mu^2}\right)} \tag{2}$$

$$\lambda = \ln\mu - \frac{1}{2}\zeta^2 \tag{3}$$

Figs.11 to 14 also show the probability density given by Equation 1, where the values of ζ and λ are computed from Equations 2 and 3 respectively, for three discrete N-values. It may be noted that the probability density tends to be representative of the distribution of the data around the discrete N-values considered.

Nominal Resistance Components

It is customary to define the nominal resistance as some fraction of the mean value (1). That is the mean value is divided by a constant factor k_R. Becker (1) recommends a value of k_R equal to 1.1 for the analysis using the static loading test results. For this study, it was decided to define the nominal resistance as the value that has at least a 70% confidence of not exceeding the measured value, in addition to satisfying the condition of k_R equal to 1.1 or more. The relations for the nominal resistance components q_n, τ_{sn}, τ_{cn} and τ_{hn} with 70% confidence of not exceeding the measured value are also shown in Figs.11, 12, 13 and 14 respectively. The value of k_R was then computed in each case by dividing the mean equations by the nominal equations, giving k_R in terms of N_P, N_S, N_C and N_h respectively. The values of k_R are plotted in Fig.15, from where the applicable range of nominal resistance components q_n, τ_{sn}, τ_{cn} and τ_{hn} satisfying the condition of k_R1.1 was obtained as N_P30, N_S30, N_C15 and N_h8 respectively.

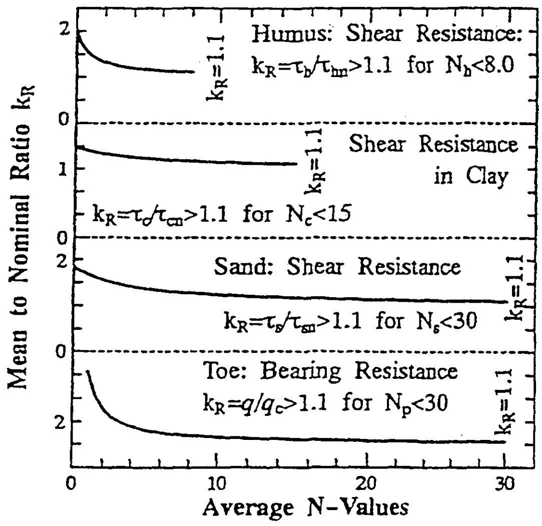

Fig.15 Range Values of N_P, N_S, N_C and N_h Satisfying the Condition of k_R1.1

Finally the relations for the nominal resistance components in *kPa* applicable within the given N-value limits were obtained. The corresponding nominal resistance relations are:

$$q_n = 155 \times N_P \quad (kPa), \quad N_P \leq 30 \tag{4}$$

$$\tau_{sn} = 24.0 + 6.0 \times N_S \quad (kPa), \quad N_S \leq 30 \tag{5}$$

$$\tau_{cn} = 24.0 + 5.3 \times N_C \quad (kPa), \quad N_C \leq 15 \tag{6}$$

$$\tau_{hn} = 5.0 + 5.2 \times N_h \quad (kPa), \quad N_h \leq 8 \tag{7}$$

$$R_n = \frac{\pi D^2 q_n}{4} + \pi D_b \sum \{\tau_{sn} \times L_s + \tau_{cn} \times L_c + \tau_{hn} \times L_h\} \quad (kN) \tag{8}$$

Computation of the Nominal Resistance

The correlation equations (4) to (7) can be utilised to evaluate the nominal resistance R_n of a pile of given length at a site of given soil profile normally available in practice. Assuming the length of pile shaft in meters in contact with sand, clay and humus to be L_S, L_C and L_h respectively, and with units of D and D_b in meters, the nominal resistance R_n in kN is given by Equation 8.

Equation 8 was utilised to compute the nominal resistance of all the piles at all the test locations by simply considering the soil profile, with complete disregard to the strain gage instrumentation interval used in the loading tests. Then the agreement of the computed nominal resistance R_n was compared with the ultimate resistance directly measured from the loading test R_m by defining the ratio $\Psi_{mn}=R_m/R_n$. The distribution of the value of Ψ_{mn} is shown in Fig.16, where it can be noted that most of the value of Ψ_{mn} lie in a narrow range of 0.9 to 1.3.

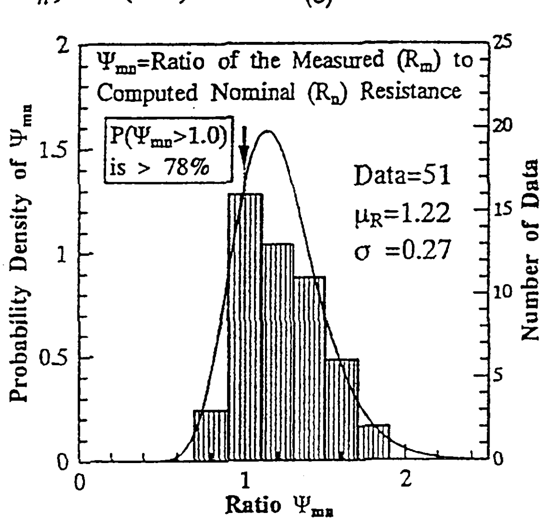

Fig.16 Distribution of the Ψ_{mn} Data and the Lognormal Distribution Approximation

RELIABILITY OF NOMINAL RESISTANCE

The Ψ_{mn} data shown in Fig.16 clearly shows a skewed distribution with a mean μ_R=1.22 and standard deviation σ=0.27, where a lognormal distribution is shown to be a reasonably close approximation. Again, the probability density of Ψ_{mn} is computed from Equation 1 with $R=\Psi_{mn}$ and λ and ζ obtained from Equations 2 and 3. Based on the lognormal distribution, the probability of Ψ_{mn} exceeding 1.0, designated as $P(\Psi_{mn}>1.0)$ in Fig.16, was found to be about 78%. It means that the nominal resistance of bored PHC nodular piles computed from Equations 4 to 8 has about 78% probability of not exceeding the resistance obtained from loading tests. It is evident that larger the chance of nominal resistance not exceeding the measured value larger the degree of safety and smaller the probability of failure.

Logically, the nominal value of the vertical resistance of a bored PHC nodular pile may be assumed to corresponds to a value of Ψ_{mn}=1.0, in which case the ratio of mean to nominal resistance k_R would be 1.22 and the coefficient of variation (COV) of the resistance $V_R=\sigma/\mu_R$ works out to be 0.22. These values may be compared to k_R=1.1 and V_R=0.25 respectively proposed (1) for analysis using static loading test results. For the purpose of the reliability analysis, a nominal resistance value of 1.0 was assumed with V_R=0.22. Current design practice in Japan involves the working stress design (WSD) method with a global factor of safety (FS) of 3.0. Considering FS=3.0 applied to the nominal resistance, the mean service load μ_S may be obtained as 0.33. The reliability index β is given by Equation 9 (1). It is known that the reliability index β gives a rational measure of the relative degree of safety, and a higher value of β means a smaller probability of failure and a higher factor of safety.

$$\beta = \frac{\ln\left\{\left(\frac{\mu_R}{\mu_S}\right)\sqrt{\left[\frac{1+V_S}{1+V_R}\right]}\right\}}{\sqrt{\ln\left[\left(1+V_S{}^2\right)\left(1+V_R{}^2\right)\right]}} \tag{9}$$

In Equation 9, V_S is the COV of load effects, which is said to range between 0.12 and 0.19, with a typical value of 0.15 (1). Assuming V_S=0.15, and with the values of μ_R, V_R and μ_S mentioned above, the reliability index is obtained as 4.9 from Equation 9. This value of β for the vertical resistance of bored PHC nodular pile is much larger than β =3.2 proposed for the axial resistance of deep foundation using the analysis based on static loading test results (1). It is seen that the nominal resistance of bored PHC nodular piles estimated from Equation 8 can be utilised with a good margin of reliability as per the current design practice in Japan.

Conversely, it was found that the FS applied to the nominal resistance R_n obtained from Equation 8 to arrive at the mean service load may be reduced to 2.0 if a reliability index of 3.2 is considered acceptable. If the designer is to be provided with the option to select a suitable FS based on local situation particular to a site, rather than specifying a single FS of 3.0 in all cases, a minimum global FS of 2.0 may be specified for the control of the vertical bearing resistance of the bored PHC nodular piles.

CONCLUSIONS

The bearing resistance of bored PHC nodular pile is derived from the transfer of load to the surrounding soil by the hardened cement grout. Analysis of the compressive strength test data indicate over 95% confidence of exceeding the target design strength of grout. It is also confirmed by completely pulling out the bored PHC nodular pile that the strength of the grout actually hardened within the ground exceeds the target strength. These investigations demonstrate the installation reliability of bored PHC nodular piles.

The comparison of the results of head loading, toe loading and shaft loading tests, utilising the Osterberg cell in combination with the reaction frame system, indicate that the head loading with strain gage measurement provides reliable separation of the total capacity into shaft resistance and toe resistance components. The toe and shaft movement curves, obtained directly from the toe loading and the shaft loading respectively, compare well with those obtained from head loading and strain gage measurement. It shows the effect of interaction between shaft and toe movement during the head loading is small in bored PHC nodular piles. This may be because the overall movement of the pile is dominated by shaft movement.

It is common to install a bored PHC nodular pile either by an ordinary auger with full soil displacement from the drilled hole, or by a special auger designed to reduce the volume of displaced soil to be disposed off. The reduction in displaced soil volume results from compaction of surrounding soil while drilling and may be expected to result in the increase in shaft resistance. Results of shaft loading test on a pair of piles indicate some increase in shaft resistance at larger shaft movements. But the increase is found to be quite insignificant at movement ranges representative of service load situations. As result, the potential increase in shaft resistance due to reduction in the displaced soil volume was disregarded in the formulation developed in this study.

A comprehensive loading test data on fully instrumented bored PHC nodular piles at diverse site conditions throughout Japan is analysed in detail to develop a practical and convenient approach to evaluate the vertical resistance. Concise formulations for nominal resistance components in terms of the soil parameters readily available from common exploration boring practice in Japan are proposed. The nominal resistance components are defined as having 70% confidence of not exceeding the measured resistance, while at the same time satisfying the condition of

$$K_r \geq 1.1$$

based on which the N-value range of applicability of the formulations are defined.

The reliability index β of the proposed formulation considering the practice of using a global factor of 3.0 in Japan works out to be about 4.9, much higher than 3.2 generally recommended in such case. When β of 3.2 is considered acceptable, a global factor of safety of 2.0 is found to be adequate. If the designer is to be provided with the option to select a suitable factor of safety based on local situation particular to a site, rather than specifying a single safety factor all cases, it would seem rational to specify a minimum safety factor of 2.0 for the design of bored PHC nodular piles based on the formulations proposed in this study.

It may be noted that the formulations proposed in this paper are based on simple regression analysis where the effects inherent to the variability of N-values is disregarded. A more rigorous analysis may be carried out by considering the COV of N-values while developing the correlation equations for nominal resistance components of the bored PHC nodular pile.

REFERENCES

1. BECKER D. E. Eighteenth Canadian Geotechnical Colloquium: Limit States Design for Foundations, Part II. Development for the National Building Code of Canada. Can. Geotech. J. 33: 984-1007, 1996, pp984-1007.
2. HORIGUCHI H. and KARKEE M. B. Load Tests on Bored PHC Nodular Piles in Different Ground Conditions and The Capacity Based on Simple Soil Parameters, AIJ Journal of Architecture and Building Science, No. 1, 89-94, Dec. 1995, pp89-94.
3. JGS JSSMFE Standard for Vertical Load Tests of Piles, JSF, 1990, pp1811-1933
4. OSTERBERG J. O. A New Simplified Method for Load Testing Drilled Shafts, Foundation Drilling, ADSC, 1984, pp9-11.
5. YABUUCHI S. and HIRAYAMA H. Bearing Mechanism of Nodal Piles in Sand, Deep Foundations on Bored and Auger Piles (BAP) II (Ed. W. F. Van Impe), A. A. Balkema, 1993, pp333-336.